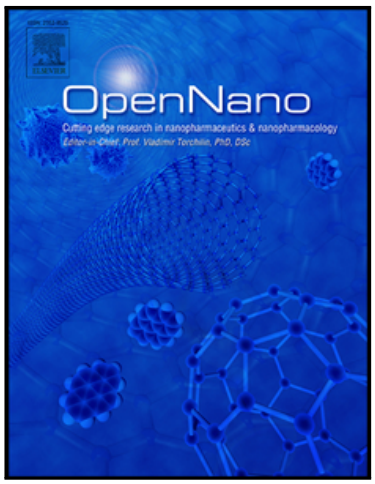

PAMAM dendrimers of generation 4.5 loaded with curcumin interfere with α-synuclein aggregation

Daniela E. Igartúa , Florencia González-Lizárraga , Carolina S. Martinez , Silvia del V. Alonso , César L. Ávila , Rosana Chehín , Nadia S. Chiaramoni , M. Jimena Prieto

PII: S2352-9520(23)00019-1
DOI: https://doi.org/10.1016/j.onano.2023.100140
Reference: ONANO 100140

To appear in: *OpenNano*

Received date: 30 December 2022
Revised date: 3 March 2023
Accepted date: 7 March 2023

Please cite this article as: Daniela E. Igartúa , Florencia González-Lizárraga , Carolina S. Martinez , Silvia del V. Alonso , César L. Ávila , Rosana Chehín , Nadia S. Chiaramoni , M. Jimena Prieto , PAMAM dendrimers of generation 4.5 loaded with curcumin interfere with α-synuclein aggregation, *OpenNano* (2023), doi: https://doi.org/10.1016/j.onano.2023.100140

PAMAM dendrimers of generation 4.5 loaded with curcumin interfere with α-synuclein aggregation

Daniela E. Igartúa[1,†,*], Florencia González-Lizárraga[2,†], Carolina S. Martinez[1], Silvia del V. Alonso[1], César L. Ávila[2], Rosana Chehín[2], Nadia S. Chiaramoni[1], and M. Jimena Prieto[1.]

[1] Universidad Nacional de Quilmes, Departamento de Ciencia y Tecnología, Laboratorio de Bio-Nanotecnología (LBN), Roque Sáenz Peña 352, Bernal, Buenos Aires, Argentina / Grupo de Biología Estructural y Biotecnología, Instituto Multidisciplinario de Biología Celular, Consejo Nacional de Investigaciones Científicas y Técnicas, CICPBA, UNLP, La Plata, Buenos Aires, Argentina.

[2] Instituto de Investigación en Medicina Molecular y Celular Aplicada (IMMCA) (CONICET-UNT-SIPROSA), Pasaje Dorrego 1080, San Miguel de Tucumán 4000, Argentina.

† These authors contributed equally to this work.

* Corresponding author: Daniela E. Igartúa, Ph.D. – daniela.igartua@unq.edu.ar – Present Address: Universidad Nacional de Quilmes, Departamento de Ciencia y Tecnología, Laboratorio de Investigación en Funcionalidad y Tecnología de los Alimentos (LIFTA), Roque Sáenz Peña 352, Bernal, Buenos Aires, Argentina / Consejo Nacional de Investigaciones Científicas y Técnicas, Godoy Cruz 2290, Ciudad Autónoma de Buenos Aires, Argentina. – Tel. (+54 11) 4365 7100 ext. 5615

Authors:

Florencia González-Lizárraga, Ph.D. – florencia.gonzalezlizarraga@fbqf.unt.edu.ar

Carolina Soledad Martinez, Ph.D. – carolinasmartinez@gmail.com

Silvia del Valle Alonso, Ph.D. – silviadelvalle@gmail.com

César L. Ávila, Ph.D. – cesar.avila@fbqf.unt.edu.ar

Rosana N. Chehín, Ph.D. – rosana.chehin@fbqf.unt.edu.ar

Nadia S. Chiaramoni, Ph.D. – nschiara@gmail.com

María Jimena Prieto, Ph.D. – jimeprieto@gmail.com

Conflicts of interest

All authors declare that they have no conflict of interest.

Acknowledgments

FGL is grateful for the fellowships granted by the Consejo Nacional de Investigaciones Científicas y Técnicas (CONICET). DEI, MJP, NSC, SdVA, CSM, CLA, and RNC are members of the Scientific Research Program from the CONICET. Also, we thank the cell bank of the Instituto Multidisciplinario de Biología Celular (IMBICE) for the generous donation of the Neuro-2a cell line.

Funding

This work was supported by National University of Quilmes grants PUNQ 1311/19 and PUNQ 1369/17, Tucumán National University grant PIUNT D644/1, and the Scientific and Technological Promotion National Agency of Argentina PICT-2020-SERIEA-02255.

Counts:

Word count for the abstract: 145

Word count for complete manuscript (to include body text and figure legends): 5883

Number of references: 69

Number of figures: 7

Credit Author Statement

Daniela E. Igartúa[†]: Conceptualization, Methodology, Investigation, Data curation, Validation, Formal analysis, Writing - original draft, Writing - review & editing.

Florencia González-Lizárraga[†]: Conceptualization, Data curation, Methodology, Investigation, Formal analysis, Writing - original draft, Writing - review & editing.

Carolina S. Martinez: Methodology, Validation, Investigation.

Silvia del V. Alonso: Supervision, Funding acquisition, Project administration.

César L. Ávila: Validation, Formal analysis, Supervision, Funding acquisition, Project administration, Writing - review & editing.

Rosana Chehín: Supervision, Funding acquisition, Project administration.

Nadia S. Chiaramoni: Supervision, Funding acquisition, Project administration.

M. Jimena Prieto: Conceptualization, Supervision, Funding acquisition, Project administration.

Abstract

Curcumin (CUR) is a bioactive compound that has been proposed for the treatment of various neurodegenerative diseases. However, its use is limited due to its low solubility in aqueous media and chemical instability under physiological conditions. Herein, we propose a strategy to overcome these limitations by using PAMAM dendrimers of generation 4.5 (DG4.5). Using a combination of biophysical techniques together with *in vitro* models, we demonstrate that CUR-DG4.5 complexes: (i) increased the solubility and stability of CUR via internalization into dendrimer's pockets and interaction with terminal carboxylic groups; (ii) showed *in vitro* biocompatibility and increased CUR uptake; (iii) presented DPPH radical scavenging activity and *in vitro* inhibition of H_2O_2-induced stress; and (iv) interfere with α-synuclein aggregation. In conclusion, this work lays the foundation to use curcumin-loaded PAMAM dendrimers of generation 4.5 as nanodrugs capable of reducing oxidative stress and inhibiting α-synuclein aggregation to treat synucleinopathies.

Keywords: Curcumin, PAMAM dendrimers, α-synuclein aggregation, antioxidant activity, Parkinson´s disease.

1. Introduction

Parkinson's disease (PD) is a chronic, progressive neurodegenerative disease traditionally described as a movement disorder, although non-motor symptoms are also observed. Histopathologically, it is characterized by the loss of dopaminergic neurons in the *substantia nigra*, along with α-synuclein deposits into Lewy bodies and Lewy neurites [1], increased levels of oxidative stress, and neuroinflammation [2,3]. To date, there is no pharmacological treatment to stop the progression of the disease. Taking into account that by 2040 the prevalence of PD is expected to rise to 12 million people [4], it is imperative to develop disease-modifying therapies that prevent or delay the disease progression. The design of new treatments requires considering the multifactorial nature of the disease and generating multi-interventional strategies to prevent or decrease its progression, targeting α-synuclein aggregation, oxidative stress, and neuroinflammation.

Curcumin (CUR) is a natural polyphenol that is derived from *Curcuma longa,* an herbaceous root native from Southeast Asia [5]. It has been proven to be safe in high doses in humans and is generally used as a spice and food coloring and as a medicine in Oriental and Ayurvedic practices. Due to its antioxidant [6], anti–inflammatory [7], free radical scavenging [8], mitochondrial protecting [9], and iron-chelating properties

[10]. [illegible] treatment of PD. Furthermore, CUR has been shown to inhibit monoamine oxidase activity, which could enhance dopaminergic levels in the brain [12], and to modulate alpha-synuclein mediated toxicity by binding to preformed aggregates [13]. Altogether, this data has encouraged the scientific community to pursue preclinical [14] and clinical studies [15] to evaluate the potential of CUR for the treatment of PD. Unfortunately, these efforts have been hindered by its low bioavailability. In particular, low oral absorption, rapid metabolization, and high elimination rate of the system contribute to the low bioavailability of CUR [16]. Additionally, its poor water solubility and its instability in physiological conditions, constitute other challenges to be overcome. Over the years, many drug delivery systems have been proposed to overcome these limitations [17].

Dendrimers are synthetic polymers that present unique properties in the field of drug delivery systems since they have minimal polydispersity, defined surface groups, globular shape, and controlled nanometric size. Mainly, polyamidoamine (PAMAM) dendrimers of generation 4.5 (DG4.5) are optimal delivery systems because they have high water solubility and are capable of encapsulating small drug molecules into their internal pockets and/or anchoring both small and large drug molecules to their surface groups through ionic interactions [18,19]. Consequently, the drug complexed in dendrimers would acquire their physicochemical properties, which would increase its solubility in aqueous media and, as a result, modify its pharmacokinetic profile and biodistribution.

Moreover, it has been recently shown that dendrimers could have intrinsic activity and act as drugs *per se*, exhibiting anti-protein aggregation, anti-viral, anti-bacterial, and anti-inflammatory properties [20–22]. Indeed, PAMAM dendrimers can be considered nanodrugs, because they have properties as inhibitors of acetylcholinesterase [23,24], as inhibitors of β-amyloids aggregation [25,26], as anti-microbial and anti-inflammatory [27,28]. Hence, it is important to consider PAMAM dendrimers not only as delivery systems but as nanodrugs *per se*, which could act in combination with other bioactive agents in the treatment of PD.

In this work, we develop and characterize a CUR delivery system based on PAMAM dendrimers of generation 4.5. Then, related to the treatment of PD, we study the activity of our delivery system to inhibit the oxidative stress process and α-synuclein aggregation.

2. Materials and methods

2.1 Materials

Curcumin (CUR, CAS N°458377) was from Santa Cruz Biotechnology (Texas, USA). Polyamidoamine (PAMAM) dendrimer of generation 4.5 (DG4.5, CAS N°470457) was acquired from Sigma-Aldrich (Missouri, USA). The commercial methanolic suspension (purity >99%) was stored at 4 °C, as recommended by the supplier, and used without additional purifications. Tetrazolium MTT salt was from USB Corporation; MEM was from HyClone; the antibiotic-antimycotic 100X and trypsin 10X solutions were from Gibco (Thermo Fisher Scientific). The FBS was from Internegocios S.A. (Buenos Aires, Argentina).

Gie

and 2,2-Diphenyl-1-(2,4,6-trinitrophenyl)hydrazyl (DPPH) were acquired in Sigma-Aldrich. Finally, neutral red dye (NR) was from BioPack (Buenos Aires, Argentina). The remaining chemicals were analytical grade.

2.2 CUR-DG4.5 complexation process

Different amounts of CUR were combined in a methanolic solution with a constant amount of DG4.5 to determine the optimum CUR:DG4.5 ratio. The molar ratios were 2:1, 5:1, 10:1, and 25:1, corresponding to 0.048, 0.12, 0.24, or 0.6 mM of CUR and 0.024 mM of DG4.5, respectively. The mixtures (n=3) were incubated under constant stirring in the dark for 24 h at 28 °C, and then methanol was evaporated at 25 °C in a SAVANT® AES1010 SpeedVac concentrator (Thermo Fisher Scientific, USA). The remaining solids were resuspended in 10 mM phosphate buffer saline at pH=7.4 (PBS). The samples were centrifuged at 10000 rpm for 5 minutes to separate the insoluble free CUR from the DG4.5 or CUR-DG4.5 complexes in suspension (Fig. S1). The complexation protocol was repeated (n=16) to study its reproducibility.

2.3 CUR quantification

The quantification of CUR was carried out by monitoring its maximum absorbance peak at 424 nm in dimethyl sulfoxide (DMSO) (Fig. S2 A) using a Cytation 5 spectrophotometer (BioTek Instruments, USA). The equation of the calibration curve was obtained by linear regression (R^2=0.9928) in a concentration range of 1-530 µM (n=6). The CUR incorporated into DG4.5 was quantified by an indirect method (Fig. S3).

2.4 CUR-DG4.5 complexes characterization and stability studies

2.4.1 Fourier Transformed Infrared (FTIR) Spectroscopy

Suspensions of CUR and CUR-DG4.5 were frozen at -80 °C overnight and then lyophilized for 24 h in a LABCONCO Freezone® 4.5 lyophilizer. The solid samples were analyzed using a Nicolet 8700 FTIR spectrometer (Thermo Fisher Scientific, USA) and the attenuated total reflectance technique, after 64 scans in the wavenumber range from 1250 to 4000 cm^{-1}, with a resolution of 2 cm^{-1}.

2.4.2 ζ-potential and size distribution

Suspension of CUR-DG4.5 and DG4.5 were examined at 25 ± 2 °C with a Zetasizer Nano ZSP ZEN 5600 analyzer (Malvern Instrument, UK). The refractive index was set to 1.45 for DG4.5 and CUR-DG4.5 complexes, and 1.33 for the dispersant.

2.4.3 UV-visible Spectroscopy

UV-vis absorption spectra of CUR, CUR-DG4.5, and DG4.5 were obtained with the NanoDrop™ 1000 UV-Vis spectrometer (Thermo Fisher Scientific, USA). The resolution of the instrument was 2 nm, and the wavelength range was 220-700 nm.

2.4.4 Stability studies

Suspensions of CUR and CUR-DG4.5 were stored at -20, 4, or 25 °C for 0, 1, 3, 7, 15, and 30 days, and evaluated by macroscopic observations and UV-Vis spectroscopy. In the former, the presence of

amount of soluble drug and the shifts in absorbance maximum peak were analyzed. These tests were performed in triplicate (n=3) on samples obtained from different complexation processes.

2.5 CUR-DG4.5 compatibility and uptake profiles in cell culture

The effects of free CUR (0.625–10 µM), DG4.5 (0.15–2.4 µM), and CUR-DG4.5 complexes (0.625–10 µM CUR in 0.15–2.4 µM of DG4.5) on Neuro-2a cell line were analyzed after 4 or 24 h-treatments by three colorimetric methods. The viability test using crystal violet (CV) staining [29], the metabolic activity test by MTT reaction [30], and the membrane states test by neutral red (NR) uptake [31] were performed following our previously reported methods [18,19]. Besides, the *in vitro* uptake of CUR and CUR-DG4.5 complexes was determined by fluorescence spectroscopy. The maintenance of cells and methods are fully described in Supplementary Material.

2.6 CUR-DG4.5 antioxidant activity assays

2.6.1 DPPH radical scavenging

The antioxidant activities of CUR,CUR-DG4.5, and DG4.5 were measured using DPPH radical scavenging activity assay according to the protocol described by Mohammadian et al. [32] with few modifications. Briefly, 100 µL of CUR (200 µM), CUR-DG4.5 (200 µM of CUR in 48 µM of DG4.5), or DG4.5 (48 µM) suspensions were placed in a 96-well plate. Then, 100 µL of ethanolic DPPH solution (0.2 mM) was added to each well. The mixtures were mixed and stored in the dark for 30 min at room temperature. The absorbance was measured at 517 nm using Cytation 5 multi-plate reader. The DPPH radical scavenging activity was calculated according to Equation 1.

$$Radical\ scavenging\ activity\ (\%) = \frac{Abs_{control} - (Abs_{sample} - Abs_{blank})}{Abs_{control}}\ x\ 100 \qquad \text{Equation 1}$$

where $Abs_{control}$, Abs_{sample}, and Abs_{blank} are the absorbance of negative control (PBS with DPPH), sample (CUR,CUR-DG4.5, or DG4.5 suspension with DPPH), and blank (CUR,CUR-DG4.5, or DG4.5 suspension without DPPH), respectively. In addition, BHT at 200 µM was used as a positive control due to its well-known antioxidant activity.

2.6.2 Activity against H_2O_2-induced stress in cell culture

MTT assay was performed to determine the cytoprotective effect of CUR and CUR-DG4.5 complexes against H_2O_2-induced stress in Neuro-2A cell culture following the method described by Ghaffari et al. [33] with minor modifications. Cells were seeded in a 96-well plate ($5x10^4$ cell/well) and incubated for 24 h. On the one hand, to examine the effect of co-treatment, cells were washed and treated with 2.5-10 µM CUR or CUR-DG4.5 complexes, and 35 µM H_2O_2. On the other hand, to study the effect of pre-treatment, cells were washed and treated with 2.5-10 µM CUR or CUR-D complexes for 2 h before the addition of 35 µM H_2O_2. In both cases, after 24 h of incubation, the metabolic activity test was performed as described in section 2.5.

2.7.1 Preparation of α-synuclein

Expression and purification of recombinant human α-synuclein were performed as previously described [34]. The purity of the protein was assessed by SDS-PAGE. Monomeric α-synuclein stock solutions were prepared in PBS pH 7.4. Before measurements, protein solutions were filtered and centrifuged for 30 min at 12000×g. Protein concentration was determined by the measurement of absorbance at 280 nm using extinction coefficient ε_{275} = 5600 cm^{-1} M^{-1}.

2.7.2 Protein aggregation

The aggregation protocol was adapted from previous studies [35]. Briefly, monomeric α-synuclein solutions (70 μM), were incubated in a Thermomixer comfort (Eppendorf) at 37 °C under orbital agitation at 600 rpm either in the absence or in the presence of CUR (100 μM), DG4.5 (24 μM), or CUR-DG4.5 complexes (100 μM CUR in 24 μM of DG4.5).

2.7.3 Congo red assay

The formation of a cross-β structure during aggregation was followed by the addition of Congo Red on aliquots withdrawn from the incubation mixture at different times, according to Klunk et al [36,37]. Changes in the absorbance spectra were monitored in a TECAN multiplate reader using a 96-well plate. The amount of fibril was estimated following Equation 2.

$$c = \frac{OD_{540}}{25295} - \frac{OD_{477}}{46306} \qquad \text{Equation 2}$$

2.7.4 Transmission Electron Microscopy

Aliquots taken from protein aggregation were adsorbed onto glow-discharged 200 mesh formvar carbon coated copper grids (Electron Microscopy Sciences) and stained with 2% uranyl acetate. Excess liquid was removed, and grids were allowed to air dry. Images were captured using a Libra 120 (Carl Zeiss) transmission electron microscope.

2.7.5. Cytotoxicity assay

SH-SY5Y cells were grown in DMEM supplemented with 10% fetal bovine serum (FBS) and 1% penicillin/streptomycin (PS), at 37 °C and 5% CO_2. For cytotoxicity assay cells were seeded in 96 wells plates at 20000 cells/well and maintained in 100 µl of DMEM supplemented with 10% FBS and 1% PS for 24 h at 37 °C. Afterwards, cells were treated with a PBS buffer, pH 7.4 (NT), α-synuclein oligomers, fibrils, and the other species formed in presence of curcumin and dendrimer. After treatment, cells were incubated for 24 h at 37 °C 5 % CO_2 and to determine cytotoxicity was determined using the Cytotoxicity Detection Kit (Roche) following instructions from the manufacturer. The assay is based on the measurement of the activity of lactate dehydrogenase (LDH) released into the culture medium upon permeabilization or lysis of cells. Percentage of cytotoxicity is referred to the LDH activity released from cells after treatment with 1%

Trit

expressed as a percentage relative to the untreated cell control.

2.8 Statistical analyses

All measurements are expressed as the mean ± the standard deviation. The statistical analyses were performed using the Graph Pad Prism v8.0 program. Depending on the experimental design, T-test, One-way ANOVA, or Two-way ANOVA were used, followed by corresponding multiple comparisons post-test. In all cases, only when the p-value was less than 0.05, the differences were considered significant. The degree of significance was represented with asterisks, such as * $p<0.05$, ** $p<0.01$, *** $p<0.001$, and **** $p<0.0001$. The abbreviation *ns* was used to express not significant differences.

3. Results and discussion

3.1 CUR complexation into DG4.5

Curcumin (CUR) is a bioactive compound that could be used for the treatment of neurodegenerative diseases, including Parkinson´s Disease (PD). However, its use is limited due to its poor water solubility (0.6 µg/mL, 1.63 µM, at 25 °C), its instability under physiological conditions (short half-life), and its low bioavailability [16,38,39]. In this sense, PAMAM dendrimers arise as good candidates to manage these limitations, through interactions that depend on the characteristics of the nanomaterial, the bioactive compound, and the conditions of the medium [40,41]. Therefore, we aimed to obtain and characterize complexes between CUR and PAMAM DG4.5 to study if this dendrimer could increment the solubility and stability of this bioactive compound.

The ability of DG4.5 to complex the CUR was evaluated by exposing different amounts of the drug to a constant amount of dendrimer in methanolic solution and applying a drying and resuspension-in-buffer processes (Fig. S1). The concentration of soluble CUR was measured by an indirect method (Fig. S3). The concentrations of soluble CUR in the CUR-DG4.5 complexes were significantly higher than those obtained for CUR in absence of dendrimer (Fig. 1A). In addition, the increment of CUR:DG4.5 molar ratio enhanced the amount of CUR interacting with dendrimers (Fig. 1C). It should be noted that the concentration of soluble CUR in the absence of the dendrimer measured by the indirect method is higher than the concentration expected from the reported solubility (1.6 µM). This disagreement could be explained by the existence of a degradation phenomenon. The CUR degradation could occur during the incubation period of CUR methanolic solution and/or during the drying process. In this sense, D'Archivio and Maggi (2017) studied the stability of curcumin in water-methanol mixtures showing that, although the increment in methanol concentration improved the stability of curcuminoids, the half-life times still being very low (3.8 ± 0.2 h) [42]. In addition, Chemroenphat et al. (2021) investigated the freeze drying, hot air drying, and sun drying effects on curcuminoids compared with fresh turmeric, showing that curcuminoids degradation to ferulic acid and vanillin occurs in all drying processes [43]. Particularly, in CUR concentration equivalent to 25:1 CUR:DG4.5 molar ratio, a considerable amount of degraded CUR was observed (reflected in the

res

be reduced or even inhibited during the complexation with DG4.5 due to the drug-dendrimer interaction, since it was reported that CUR degradation was significantly decreased when the drug is interacting with lipids, liposomes, albumins, cyclodextrin, surfactants, polymers and many other macromolecular and microheterogenous systems [44]. Therefore, in the search for a balance between increasing the concentration of CUR in aqueous media, without losing it by degradation, we selected the 10:1 CUR:DG4.5 theoretical molar ratio to study the reproducibility of the complexation process.

At 10:1 CUR:DG4.5 molar ratio, the formation of CUR-DG4.5 complexes allowed a significant increase in CUR solubility in aqueous media (Fig. 1B). In the free CUR control, an average resuspension of 37.77 ± 6.38 µM was obtained. As the solubility of the drug in water is 1.6 µM [45], we can assume that the difference between these values is the amount of degraded CUR during the complexation process. In the CUR-DG4.5 complexes, the CUR concentration was 105.5 ± 17.7 µM. In this case, we cannot confirm that the drug is degraded as in the CUR control since dendrimers stabilized the CUR during the solvent evaporation step of the complexation process (Fig. S4). As the concentration of dendrimer in suspension was known, we calculated the experimental CUR:DG4.5 ratio, which resulted in an average of 4 ± 1 moles of CUR per mole of DG4.5 (Fig. 1 D). Our results are consistent with those reported by Markatou et al. [5], who studied the incorporation of demethoxycurcumin in PAMAM DG3.5 and DG4.0 and reported that an initial 1:8 and 1:10 dendrimer:demethoxycurcumin ratios were necessary to achieve the maximum incorporation of 4.2 and 5.0 CUR molecules per molecule of DG3.5 or DG4.0, respectively.

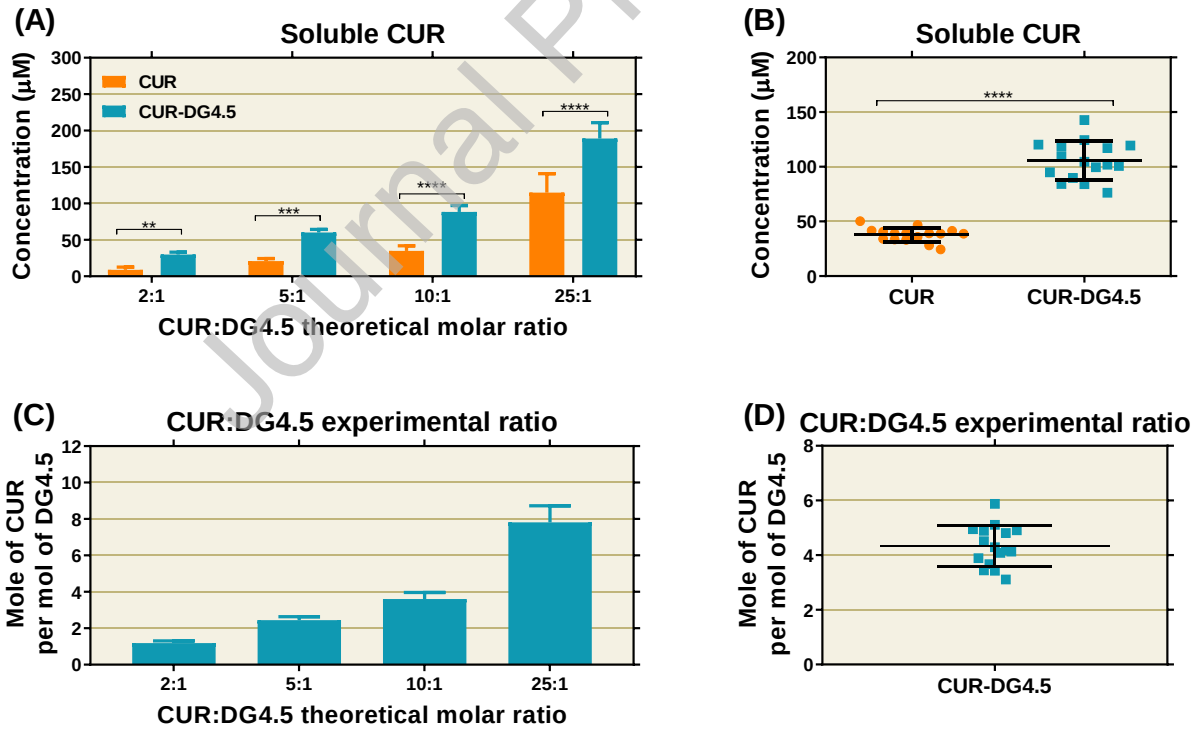

Fig. 1 – Optimization of CUR-DG4.5 complexation. Concentration of soluble CUR after complexation process using CUR:DG4.5 molar ratios **(A)** from 2:1 to 25:1 (n=3) and **(B)** 10:1 (n=16). Mole of CUR per mole of DG4.5 after complexation process using CUR:DG4.5 theoretical molar ratios **(C)** from 2:1 to 25:1 (n=3) or **(D)** 10:1 (n=16).

3.2 Characterization and stability of CUR-DG4.5 complexes

Chemically, CUR is a compound that has two phenolic hydroxyls and a β-diketone-α-β-unsaturated domain in its structure. This domain presents keto-enol equilibrium in solution, being able to find three tautomers (diketo, keto-enol, or dienol) in different proportions depending on the solvent and temperature [46,47]. The diketo tautomer has two antiparallel ketone groups, which gives an angular arrangement and two non-conjugated feruloyl fragments to the molecule, while the keto-enol tautomer presents a ketone group and an alcohol group, which generates a completely conjugated and planar structure. The maximum absorbances of the diketo and keto-enol forms were reported at 350-365 nm and 420-430 nm, respectively [48,49]. The diketo tautomer predominates in aqueous media at acidic or neutral pH and is recognized as the medicinally active tautomer, while the keto-enol predominates in organic solvents, water at alkaline pH, and solid-state samples [50,51]. In this work, the CUR tautomeric state and the interactions with DG4.5 were characterized by FTIR spectroscopy, ζ-potential analyses, size distribution studies, and UV-Vis spectroscopy.

Regarding FTIR spectroscopy, the spectrum of the CUR (Fig. 2A) presented the drug-specific absorption bands [52,53]. These include the stretching bands of the –CH and –OH bonds at 3507 cm^{-1}, the vibration of the –C=O at 1626 cm^{-1}, the stretching of the –C=C– bonds of the aromatic rings at 1601 cm^{-1}, the vibration of the –C-OH bond at 1455 cm^{-1} and the $–CH_3$ bond at 1427 cm^{-1}, and the stretching of –OH at 1315 and 1272 cm^{-1}. In this solid-state control, CUR was in its keto-enol form since the carbonyl stretching vibration was presented at 1626 cm^{-1}, instead of 1715-1745 cm^{-1} which would be expected for the di-keto form [5]. Secondly, the FT-IR spectrum of DG4.5 (Fig. 2B) showed the stretching vibrations of the -N-H bonds of the amide inside the dendrimer at 3360 cm^{-1} and 1652 cm^{-1}; the stretching vibrations of the –C-C- and -C-H bonds also inside the dendrimer at 2918 and 1558 cm^{-1}; and the symmetric vibrations of the –COO of the terminal group at 1396 cm^{-1} [19]. In the FTIR spectrum of the CUR-DG4.5 complexes (Fig. 2B), the disappearance of the absorption band at 3360 cm^{-1} and the displacement of some bands towards 2960, 1642, 1548, and 1390 cm^{-1} were observed. As these signals correspond to both the internal and the terminal groups of DG4.5, the CUR molecules could be interacting with both the dendrimer's pockets and terminal groups. Also, the stretching vibration of –C=O of the CUR is presented at 1730 cm^{-1}, showing the presence of CUR in the medicinally active di-keto form in the CUR-DG4.5 complex [5].

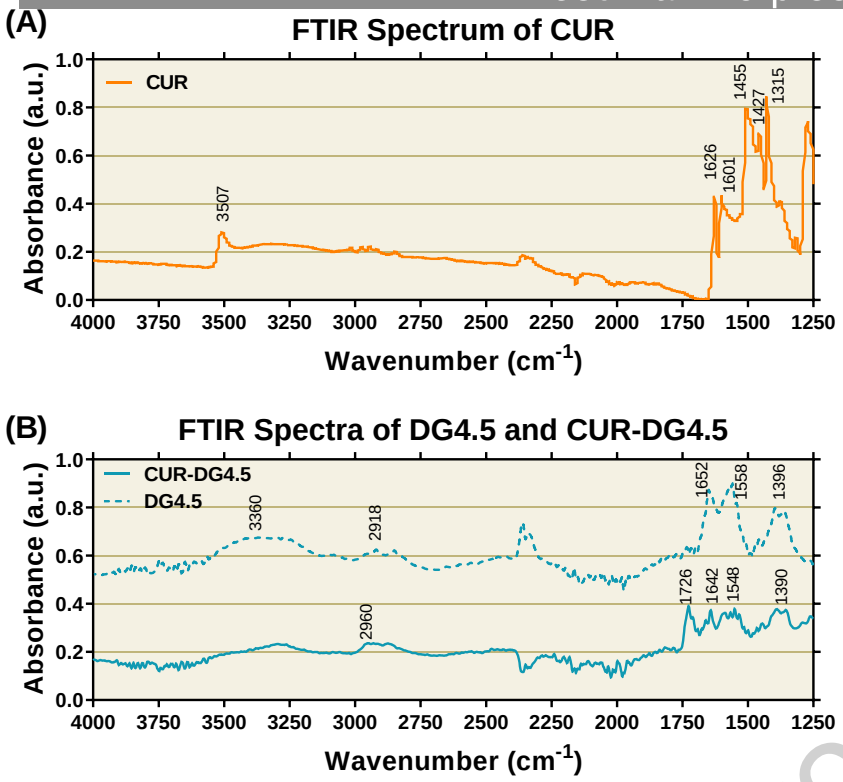

Fig. 2 – CUR-DG4.5 Characterization. FTIR spectra of **(A)** CUR, and **(B)** DG4.5 (dashed line) or CUR-DG4.5 complexes (solid line).

Concerning ζ-potential (Fig. 3A), DG4.5 presented negative ζ-potential since their terminal groups are deprotonated (COO^-, carboxylate groups) in physiological pH. The interaction with CUR reduced the ζ-potential value of CUR-DG4.5 complexes, which could be due to a dipole-anion interaction of CUR with the carboxylate groups on the dendrimer's surface. Size distribution studies using DLS show a monomodal distribution centered at 155 ± 39 nm for DG4.5 in aqueous solution, in contrast with a bimodal distribution with peaks at 146 ± 48 and 20 ± 4 nm for CUR-DG4.5 (Fig. 3B). Although the actual diameter of PAMAM DG4.5 is 4-5 nm [54], it had been previously described that dendrimers agglomerates forming nanosized particles after methanol evaporation and buffer resuspensions [55,56]. In our results, the interaction with CUR allowed the disaggregation of dendrimers into smaller particles. Both ζ-potential and size results agree with those previously described by FTIR, and with the existence of CUR-DG4.5 superficial interaction besides interaction with the internal pockets.

Regarding UV-Vis spectroscopy (Fig. 3C), CUR-DG4.5 complexes presented an initial maximum absorbance peak at 424 nm, which correlated with the keto-enol tautomer. As this form is predominant in organic solvents, the UV-Vis spectrum suggested that CUR was interacting with the low polar moieties present in the interior of dendrimers which could be approached through the external interface [16]. These results are consistent with those obtained by Cao et al [48], who studied the interaction of the CUR with PAMAM G4.0 dendrimers modified on its surface with carbonated branches (C12), which they called PAMAM-C12 25%. They reported that the CUR form complexes to its dendrimers showed maximum

abs

determined that their dendrimers had 5 binding sites for CUR, obtaining a 1:5 D:CUR molar ratio and that the complexes were stabilized by hydrophobic bonds, hydrogen bridge, and van der Waals interactions.

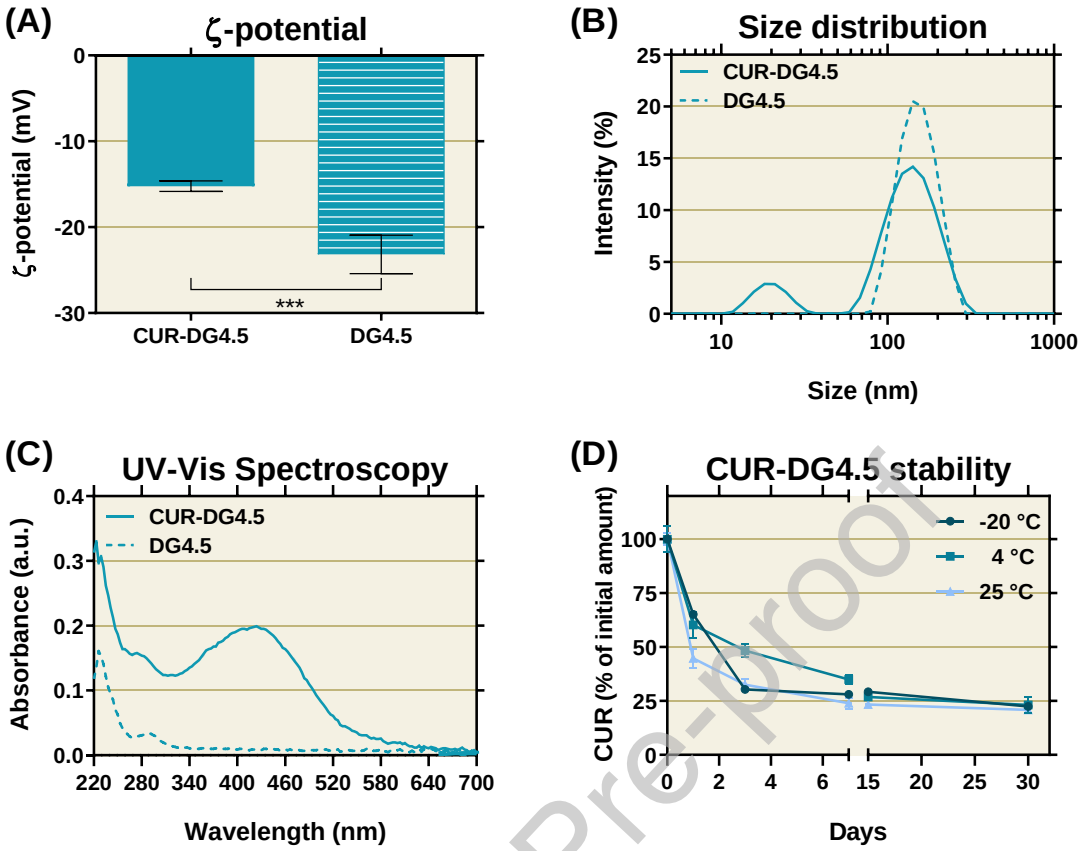

Fig. 3 – CUR-DG4.5 Characterization. (A) ζ-potential, **(B)** size distribution, and **(C)** UV-Vis absorption spectra of CUR-DG4.5 and DG4.5. **(D)** Stability of CUR in CUR-DG4.5 complexes stored at -20, 4, or 25 °C for 30 days.

Additionally, it was reported that CUR is an unstable drug that degrades to vanillin, ferulic acid, and feruloyl methane under physiological conditions [49]. Thus, it is relevant to study if dendrimers could increase the CUR stability during storage conditions. For this, CUR and CUR-DG4.5 samples were stored in darkness at -20, 4, or 25 °C for 30 days. At predetermined times, macroscopic observations were made (Fig. S5) and the UV-Vis absorbance spectra were determined (Fig. S6). Finally, the CUR half-life time was estimated as the time needed to lose 50% of soluble CUR regarding the initial amount (Fig. 3D).

Concerning the macroscopic observations of CUR-DG4.5 samples, precipitation was observed on samples stored at -20 and 4 °C, while a decrease in the color of the suspension was observed on samples stored at the three evaluated conditions (Fig. S5). Regarding UV-Vis spectroscopy, a progressive decrease in the absorbance at 424 nm and a shift to 350 nm of the maximum peak were observed as a function of time for all the storage conditions (Fig. S6). The samples stored at 25 °C showed a faster decay of CUR concentration than samples stored at -20 and 4 °C, indicating that the degradation processes were exacerbated by increasing the temperature (Fig. 3D). However, it was reported that the half-life of the CUR

is 9 [illegible] R-DG4.5 complexes was increased to ~ 3 days (72 h) for storage at -20 ° C and 4 °C, and to 1 day (24 h) for storage at 25 °C. The obtained results indicated that CUR is progressively released from the CUR-DG4.5 complexes and, while roughly 75% of released CUR is degraded or precipitated, a 25% is transformed into its medicinally active tautomer and stabilized by interaction with terminal carboxylate groups (Fig. 3D). These results are consistent with those reported by Dutta et al. (2013), who demonstrated that the di-keto CUR tautomer shows maximum absorption at 355 nm and is stabilized in aqueous media by interaction with low concentration of anionic surfactants. Also, they showed that keto-enol CUR tautomer presents a maximum absorption at 425 nm and is stabilized by interaction with the hydrophobic interior of micelles formed by anionic surfactants at concentrations above its critical micellar concentration.

Overall, the solubility of the CUR was significantly increased through interaction of the drug with both dendrimer's internal pockets and terminal carboxylate groups. It is probable that CUR partially enters the external interface of the dendrimer forming complexes due to the synergy among various types of interactions, i.e. ion-dipole, dipole-dipole, H-bonding, and Van der Waals interactions. The complexes also presented controlled-release processes of the drug that resulted in the tautomerization of the CUR to its medicinally active form.

3.3 CUR-DG4.5 compatibility and uptake profiles in cell culture

For compatibility studies, the effects of CUR, CUR-DG4.5, and DG4.5 on the viability, metabolic activity, and membrane status of the Neuro-2a cell line were studied after 4 or 24 h treatments (Fig.s S7 and S8, respectively). The treatment with CUR and CUR-DG4.5 were nontoxic. Otherwise, the 24-h treatment with the higher concentration of DG4.5 produced a reduction in NR uptake, which could mean that DG4.5 damaged the cell membrane. These results are consistent with those previously reported regarding the toxicity of CUR in cell culture. For example, Debnath et al. (2013) studied the toxicity of CUR in two breast cancer cell lines and, through the MTT test, determined that the 50% inhibitory concentration of metabolic activity (IC_{50}) of CUR was 47.9 ± 21.5 µM in SKBr3 and 35.8 ± 18.4 µM for BT549. In this sense, as we work with CUR concentrations lower than those IC50, no effects were observed at the Neuro-2a metabolic activity. Accordingly, Wang et al. (2013) studied the toxicity of CUR in A549 cells by the MTT method and demonstrated that 5 and 10 µM of free CUR produced no effect on metabolic activity. In addition to this, Lin et al. studied the effect of 2.5 µM of CUR on Neuro-2a cells and reported no toxic effects measured by MTT [58]. Therefore, the use of different detection methods, concentrations, and incubation times, allowed us to demonstrate that CUR-DG4.5 complexes did not present cytotoxic effects in the evaluated concentrations.

For the uptake profile study, the CUR fluorescence emission in cell culture was determined after 2, 4, and 24 h of incubation with CUR or CUR-DG4.5 (Fig. 4). The CUR-DG4.5 presented a significantly higher uptake of CUR than free drug control after 4 and 24 h of incubation. It is possible that the higher uptake of CUR results from the uptake of the complex into the cell through energy-dependent mechanisms, mainly by clathrin and caveolae mediated endocytosis [59–61]. Alternatively, it is also possible that the dendrimers

allo

dependent mechanisms. Finally, the dendrimers also increase the stability of the CUR, allowing a greater amount of drug to be present for a longer time for its uptake by non-energy-dependent mechanisms.

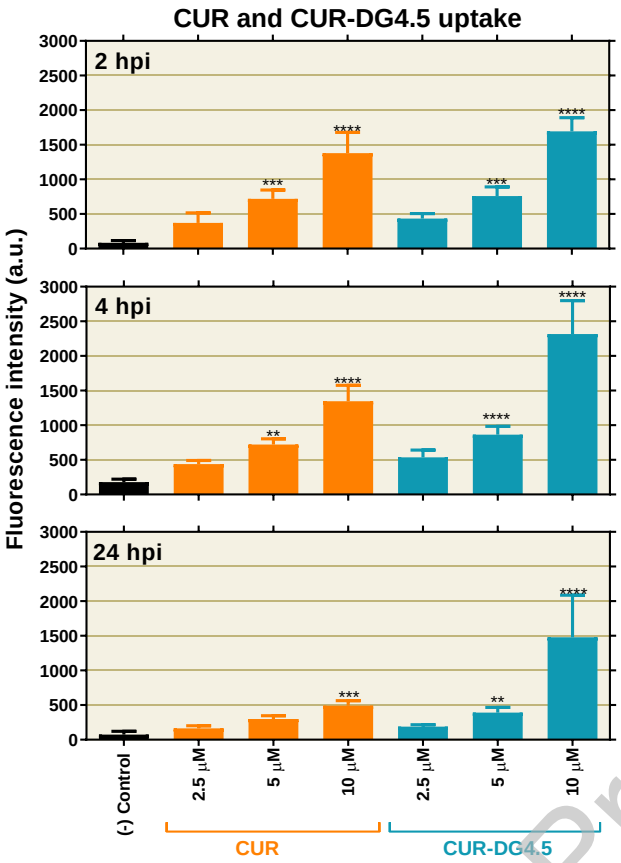

Fig. 4 – *In vitro* uptake profile. CUR fluorescence intensity in Neuro-2a cell culture after 2, 4, o 24-h treatments with CUR or CUR-DG4.5 complexes.

3.4 CUR-D antioxidant activity assays

The design of new PD treatments must address the multifactorial nature of the disease. To explore the ability of CUR-DG4.5 complexes against oxidative stress, we measured the DPPH radical scavenging activity and the *in vitro* activity against H_2O_2-induced stress in Neuro-2a cell culture.

CUR and CUR-DG4.5 presented a significantly higher DPPH radical scavenging activity than BHT positive control, whereas DG4.5 did not present significant scavenging activity (Fig. 5A). Similar results were obtained for CUR encapsulated in proteins and proteins-polysaccharide nanoparticles [32,62]. Ak & Gülçin described that DPPH radical can receive a H-radical from CUR hydroxyl group, which stop DPPH radical reactions and confer antioxidant properties to CUR [63]. In addition, both CUR and CUR-DG4.5 reduced the H_2O_2-induced stress as shown by the significant increase of the metabolic activity in the cells that were simultaneously co-treated with H_2O_2 and CUR or CUR-DG4.5 in comparison to the controls treated with H2O2 alone (Fig. 5B). However, these samples did not recover the metabolic activity observed in the

before the H_2O_2 addition, both pre-treatments allowed to recover the metabolic activity of the control treated with PBS, showing a high inhibition of H_2O_2-induced stress (Fig. 5C). Likewise, Qi et al. demonstrated that, in HTR8/SV cells, pre-treatment with 5 µM CUR alleviated H_2O_2-induced stress by improving the antioxidant capacity and activating Nrf2 signaling pathway, while Rakotoarisoa et al. demonstrated that, in SH-SY5Y cells, pretreatment with CUR loaded in cubosomes resulted in an increased number of live cells upon exposure to H_2O_2 [64,65]. Our results demonstrated that upon interacting with DG4.5, CUR did not lose its capacity to inhibit oxidative stress.

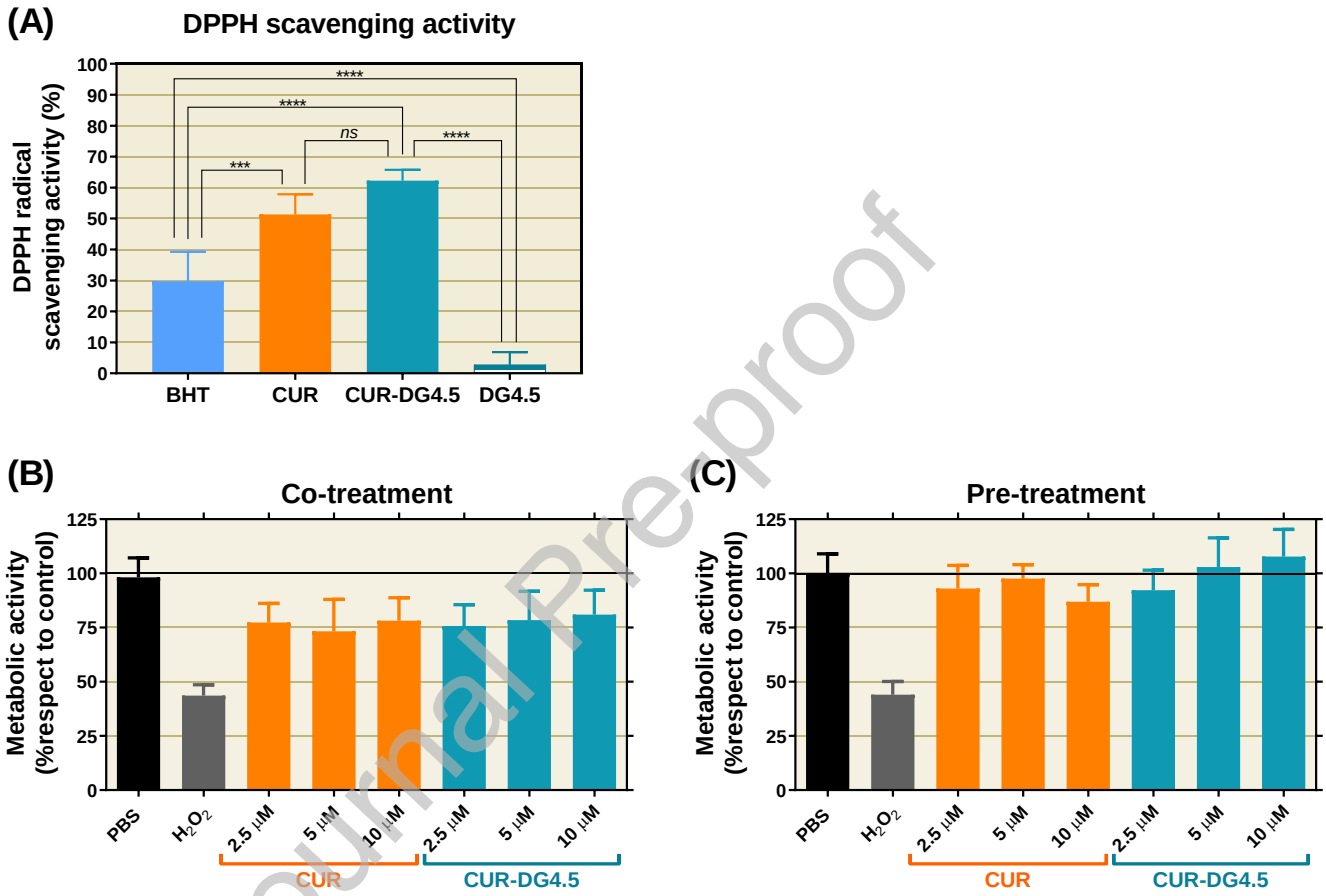

Fig. 5 – *In vitro* antioxidant activity. (A) DPPH radical scavenging activity of BHT, CUR, CUR-DG4.5, and DG4.5. Capacity of CUR or CUR-DH4.5 to inhibit H_2O_2-induced oxidative stress in Neuro-2a cell culture **(B)** during co-treatment or **(C)** by 2-h pre-treatment.

3.5 CUR-D α-synuclein aggregation assays

Finally, protein aggregation has been proposed to be a key event in the development and progression of PD. To evaluate the ability of CUR-DG4.5 complexes to interfere with the fibril assembly process of α-synuclein, amyloid-like aggregation of this protein was monitored in the absence or presence of either CUR, DG4.5, or CUR-DG4.5 using Congo Red. In this assay, fibril formation is seen as a bathochromic shift in the Congo Red emission spectra upon binding of this probe to aggregates rich in cross-β structure

exponential growth to finally reach a plateau at 48 h (Fig 6A). It should be noted that the addition of CUR to the incubation mixture results in a shortening of the *lag* phase with a concomitant increment in the total amount of fibril formed. In contrast, the presence of DG4.5 seems to affect the nucleation of α-synuclein, as shown by the extension of the *lag* phase, preventing the formation of amyloid-like fibrils. The inhibitory effect of DG4.5 on α-synuclein is retained even when loading the dendrimer with CUR. The global effect on protein aggregation after 120 h of incubation could be better appreciated in Fig. 6B. It should be noticed that while CUR increased α-synuclein aggregation, as previously reported [13], DG4.5 completely abolished α-synuclein aggregation, a property that was not disrupted by loading the dendrimer with CUR. Taking into account that CUR accelerates α-synuclein aggregation through binding only to preformed oligomers or fibrils [13], it is possible to speculate that DG4.5 dendrimers exert their inhibitory effect in previous stages of aggregation sequestering α-synuclein monomeric or early oligomeric species.

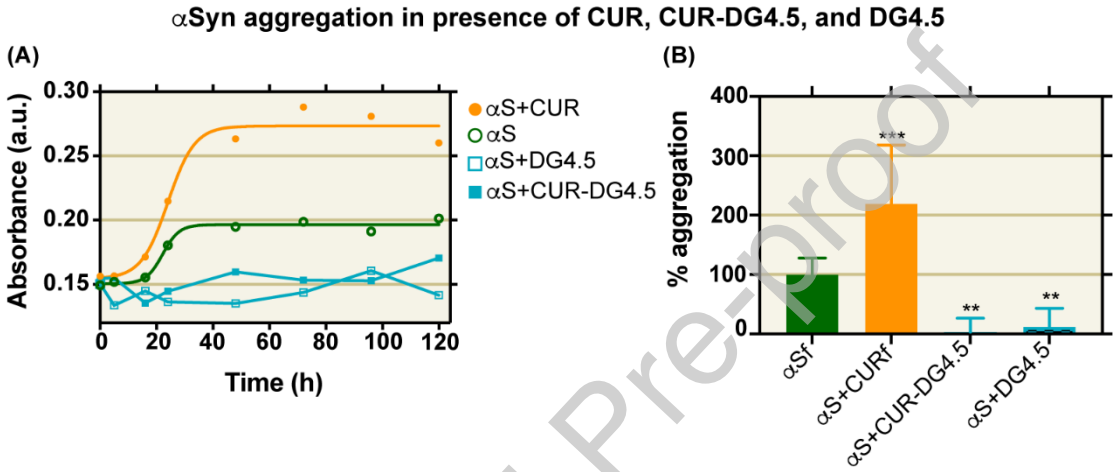

Fig. 6 - Effect of CUR, CUR-DG4.5, and DG4.5 on α-synuclein aggregation. (**A)** Aggregation kinetics of α-synuclein incubated either alone or in the presence of CUR, DG4.5, or CUR-DG4.5 monitored with Congo Red aggregation assay. (**B)** Endpoint aggregation of samples containing 70 μM α-synuclein incubated for 120 h in the absence or presence of CUR, CUR-DG4.5, or DG4.5.

To further evaluate the impact of the dendrimer on the morphology of the species present along the aggregation pathway, we performed TEM studies on samples of monomeric α-synuclein incubated alone or in the presence of CUR, DG4.5, and CUR-DG4.5 for 120h. We were able to detect fibrils when α-synuclein was incubated alone or in the presence of CUR, which were morphologically undistinguishable by TEM (Fig.s 7A and 7B). In contrast, the absence of fibrils is evident in the samples that contained either DG4.5 or CUR-DG4.5 complex (Fig.s 7C and 7D), further corroborating the lack of aggregates with cross-β structure observed using the Congo Red assay (Fig. 6A). Instead, small spherical aggregates show up with an average diameter of 77 ± 8 nm (Fig.s 7C and 7D), compatible to the size of the dendrimer observed by DLS (Fig. 3B). Even though the particle size observed for the dendrimers by TEM is smaller than the one estimated by DLS, this difference has also been observed in other systems and attributed to solvent layers attached to the dendrimers during DLS measurement [66]. At last, in the samples incubated in the

observation further reinforces the idea that DG4.5 halt α-synuclein aggregation at very early stages.

To our knowledge, this is the first time that PAMAM dendrimers with carboxylate groups at the chain-ends are shown to inhibit α-synuclein aggregation [67]. Since inhibition has also been shown to depend on the size of the dendrimers [68], perhaps the difference observed with previous reports rely on the sample preparation used in this study leading to larger interaction surface with the ability to stabilize monomeric or early oligomeric species of α-synuclein. In this way, we cannot discard that the aggregates observed in TEM images are formed by a mixture of α-synuclein and DG4.5.

Cytotoxicity of α-synuclein has been linked to both oligomeric and fibrillar species formed during protein aggregation [69]. Considering that the DG4.5 PAMAM dendrimer seems to halt the aggregation process at the early stages, it is crucial to evaluate the toxicity of the newly formed species. For this purpose, SH-SY5Y cells were incubated with α-synuclein monomers, oligomers, fibrils, or the aggregated species formed in the presence of CUR, DG4.5, or CUR-DG4.5. After a 24 h treatment, cytotoxicity was measured using a LDH assay kit. As shown in Fig. 7E, monomeric species of α-synuclein do not have cytotoxic activity. In contrast, α-synuclein oligomers severely affect cell survival, as reflected by a release of up to 30% of LDH into the media, as compared to the total amount released upon treatment with 1% Triton X-100. The toxicity of α-synuclein is hampered upon maturation of the aggregates into fibrils under our experimental conditions, as previously reported [35]. Most importantly, the aggregates formed in the presence of CUR, DG4.5, or CUR-DG4.5 do not induce a significant release of LDH from SH-SY5Y cells, suggesting that these compounds could be used to prevent α-synuclein mediated toxicity.

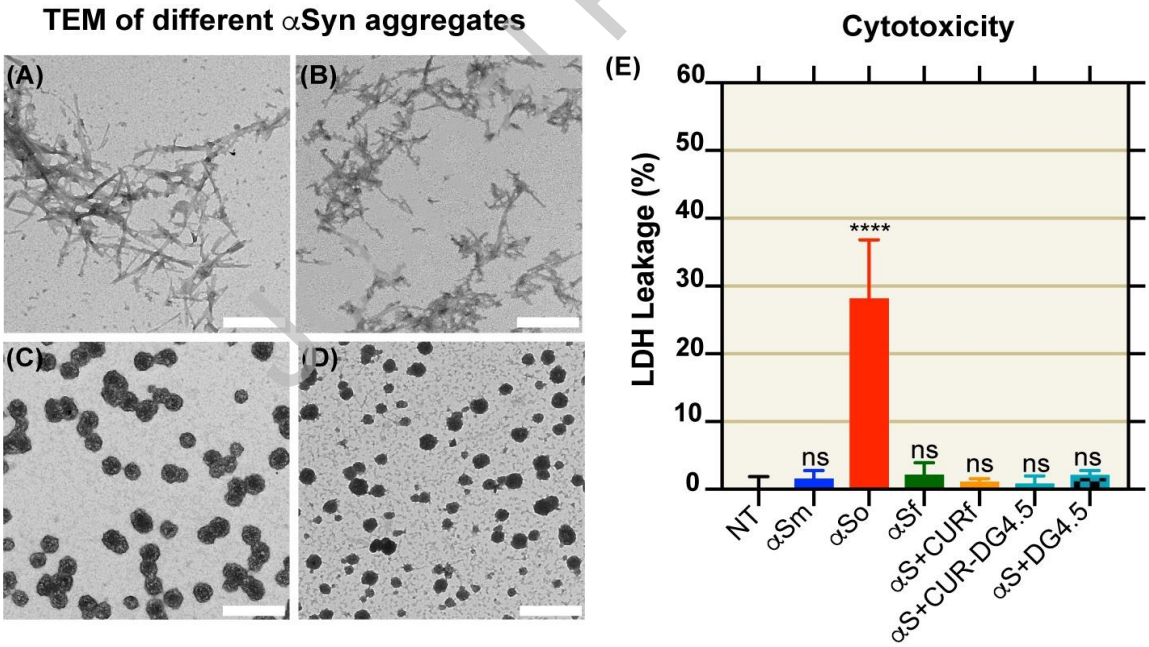

Fig. 7 - Morphology and cytotoxicity of α-synuclein aggregates. Transmission electron microscopy of α-synuclein samples incubated in the absence **(A)** or presence of CUR **(B)**, DG4.5 **(C)**, or CUR-DG4.5 **(D)** and harvested after 120 h. The scale bar corresponds to 300 nm. **(E)** LDH cytotoxicity assay in SH-SY5Y cells after the addition of α-synuclein species formed after 0 h (αSm), 16 h (αSo) or 120 h (αSf) of incubation at 37 °C under orbital agitation alone or in the presence of CUR (αS+CURf), CUR:DG4.5 (αS+CUR-DG4.5), and DG4.5 (αS+DG4.5). Cytotoxicity values were

norı

Data represents the mean ± S.E.M (n = 10). One-way ANOVA followed by Holm-Sidak's multiple comparisons test. ****p < 0.0001 vs NT.

Conflicts of interest

All authors declare that they have no conflict of interest.

4. Conclusions

In the present work, a CUR delivery system has been developed based on the complexation with PAMAM DG4.5 to obtain CUR-DG4.5 complexes. The most important expectations of this work have been fulfilled, which included increasing the solubility of the CUR in aqueous media and its stability over storage time. These factors were limiting the use of the drug in current treatments of neurogenerative disease. Moreover, CUR-DG4.5 shows high antioxidant activity measured as DPPH radical scavenging activity and inhibition of H_2O_2-induced oxidative stress in cell culture. Furthermore, DG4.5 interferes with α-synuclein pathological aggregation, which adds up to CUR's known properties for the treatment of Parkinson's disease.

References

[1] M.G. Spillantini, R.A. Crowther, R. Jakes, M. Hasegawa, M. Goedert, alpha-Synuclein in filamentous inclusions of Lewy bodies from Parkinson's disease and dementia with lewy bodies., Proc. Natl. Acad. Sci. U. S. A. 95 (1998) 6469–73.

[2] J.M. Taylor, B.S. Main, P.J. Crack, Neuroinflammation and oxidative stress: Co-conspirators in the pathology of Parkinson's disease, Neurochem. Int. 62 (2013) 803–819. https://doi.org/10.1016/j.neuint.2012.12.016.

[3] K. Hassanzadeh, A. Rahimmi, Oxidative stress and neuroinflammation in the story of Parkinson's disease: Could targeting these pathways write a good ending?, J. Cell. Physiol. 234 (2018) 23–32. https://doi.org/10.1002/jcp.26865.

[4] E.R. Dorsey, T. Sherer, M.S. Okun, B.R. Bloemd, The emerging evidence of the Parkinson pandemic, J. Parkinsons. Dis. 8 (2018) S3–S8. https://doi.org/10.3233/JPD-181474.

[5] E. Markatou, V. Gionis, G.D. Chryssikos, S. Hatziantoniou, A. Georgopoulos, C. Demetzos, Molecular interactions between dimethoxycurcumin and Pamam dendrimer carriers, Int. J. Pharm. 339 (2007) 231–236. https://doi.org/10.1016/j.ijpharm.2007.02.037.

[6] S. Abrahams, W.L. Haylett, G. Johnson, J.A. Carr, S. Bardien, Antioxidant effects of curcumin in models of neurodegeneration, aging, oxidative and nitrosative stress: A review, Neuroscience. 406 (2019) 1–21. https://doi.org/10.1016/j.neuroscience.2019.02.020.

[7] S. Ghosh, S. Banerjee, P.C. Sil, The beneficial role of curcumin on inflammation, diabetes and neurodegenerative disease: A recent update, Food Chem. Toxicol. 83 (2015) 111–124.

[8] J. Treml, K. Šmejkal, Flavonoids as potent scavengers of hydroxyl radicals, Compr. Rev. Food Sci. Food Saf. 15 (2016) 720–738.

[9] A. Salimi, Z. Jamali, L.R. Shirmard, Curcumin for protecting mitochondria and downregulating inflammation, in: Mol. Nutr. Mitochondria, Elsevier, 2023: pp. 461–500.

[10] X.-X. Du, H.-M. Xu, H. Jiang, N. Song, J. Wang, J.-X. Xie, Curcumin protects nigral dopaminergic neurons by iron-chelation in the 6-hydroxydopamine rat model of Parkinson's disease, Neurosci. Bull. 28 (2012) 253–258.

[11] C.D. Lao, M.T. Ruffin, D. Normolle, D.D. Heath, S.I. Murray, J.M. Bailey, M.E. Boggs, J. Crowell, C.L. Rock, D.E. Brenner, Dose escalation of a curcuminoid formulation, BMC Complement. Altern. Med. 6 (2006) 1–4.

[12] D.K. Khatri, A.R. Juvekar, Kinetics of inhibition of monoamine oxidase using curcumin and ellagic acid, Pharmacogn. Mag. 12 (2016) S116.

[13] in aggregation and toxicity, ACS Chem. Neurosci. 4 (2013) 393–407. https://doi.org/10.1021/cn3001203.

[14] E. El Nebrisi, Neuroprotective activities of curcumin in parkinson's disease: A review of the literature, Int. J. Mol. Sci. 22 (2021) 1–16. https://doi.org/10.3390/ijms222011248.

[15] V. Donadio, A. Incensi, G. Rizzo, E. Fileccia, F. Ventruto, A. Riva, D. Tiso, M. Recchia, V. Vacchiano, R. Infante, G. Petrangolini, P. Allegrini, S. Avino, R. Pantieri, B. Mostacci, P. Avoni, R. Liguori, The Effect of Curcumin on Idiopathic Parkinson Disease: A Clinical and Skin Biopsy Study, J. Neuropathol. Exp. Neurol. 81 (2022) 545–552. https://doi.org/10.1093/jnen/nlac034.

[16] S. Debnath, D. Saloum, S. Dolai, C. Sun, S. Averick, K. Raja, J. Fata, Dendrimer-Curcumin Conjugate: A Water Soluble and Effective Cytotoxic Agent Against Breast Cancer Cell Lines, Anticancer. Agents Med. Chem. 13 (2013) 1531–1539. https://doi.org/10.2174/18715206113139990139.

[17] R. Tabanelli, S. Brogi, V. Calderone, Improving curcumin bioavailability: Current strategies and future perspectives, Pharmaceutics. 13 (2021). https://doi.org/10.3390/pharmaceutics13101715.

[18] D.E. Igartúa, C.S. Martinez, S. del V. Alonso, M.J. Prieto, Combined Therapy for Alzheimer's Disease: Tacrine and PAMAM Dendrimers Co-Administration Reduces the Side Effects of the Drug without Modifying its Activity, AAPS PharmSciTech. 21 (2020) 110. https://doi.org/10.1208/s12249-020-01652-w.

[19] D.E. Igartúa, C.S. Martinez, C.F. Temprana, S. del V. Alonso, M.J. Prieto, PAMAM dendrimers as a carbamazepine delivery system for neurodegenerative diseases: A biophysical and nanotoxicological characterization, Int. J. Pharm. 544 (2018) 191–202. https://doi.org/10.1016/j.ijpharm.2018.04.032.

[20] S. Mignani, M. Bryszewska, M. Zablocka, B. Klajnert-Maculewicz, J. Cladera, D. Shcharbin, J.P. Majoral, Can dendrimer based nanoparticles fight neurodegenerative diseases? Current situation versus other established approaches, Prog. Polym. Sci. 64 (2017) 23–51. https://doi.org/10.1016/j.progpolymsci.2016.09.006.

[21] E. Nance, F. Zhang, M.K. Mishra, Z. Zhang, S.P. Kambhampati, R.M. Kannan, S. Kannan, Nanoscale effects in dendrimer-mediated targeting of neuroinflammation, Biomaterials. 101 (2016) 96–107. https://doi.org/10.1016/j.biomaterials.2016.05.044.

[22] D. Sepúlveda-Crespo, R. Ceña-Díez, J.L. Jiménez, M. Ángeles Muñoz-Fernández, Mechanistic Studies of Viral Entry: An Overview of Dendrimer-Based Microbicides As Entry Inhibitors Against Both HIV and HSV-2 Overlapped Infections, Med. Res. Rev. 37 (2017) 149–179. https://doi.org/10.1002/med.21405.

[23] B. Klajnert, M. Sadowska, M. Bryszewska, The effect of polyamidoamine dendrimers on human erythrocyte membrane acetylcholinesterase activity, Bioelectrochemistry. 65 (2004) 23–26.

[24] D. Shcharbin, M. Jokiel, B. Klajnert, M. Bryszewska, Effect of dendrimers on pure acetylcholinesterase activity and structure, Bioelectrochemistry. 68 (2006) 56–59. https://doi.org/10.1016/j.bioelechem.2005.04.001.

[25] T. Wasiak, M. Marcinkowska, I. Pieszynski, M. Zablocka, A.M. Caminade, J.P. Majoral, B. Klajnert-Maculewicz, Cationic phosphorus dendrimers and therapy for Alzheimer's disease, New J. Chem. 39 (2015) 4852–4859. https://doi.org/10.1039/c5nj00309a.

[26] B. Klajnert, M. Cortijo-Arellano, M. Bryszewska, J. Cladera, Influence of heparin and dendrimers on the aggregation of two amyloid peptides related to Alzheimer's and prion diseases, Biochem. Biophys. Res. Commun. 339 (2006) 577–582. https://doi.org/10.1016/j.bbrc.2005.11.053.

[27] I. Durocher, D. Girard, In vivo proinflammatory activity of generations 0–3 (G0–G3) polyamidoamine (PAMAM) nanoparticles, Inflamm. Res. 65 (2016) 745–755. https://doi.org/10.1007/s00011-016-0959-5.

[28] A.S. Chauhan, P. V. Diwan, N.K. Jain, D.A. Tomalia, Unexpected in vivo anti-inflammatory activity observed for simple, surface functionalized poly(amidoamine) dendrimers, Biomacromolecules. 10 (2009) 1195–1202. https://doi.org/10.1021/bm9000298.

[29] W. Kueng, E. Silber, U. Eppenberger, Quantification of cells cultured on 96-well plates, Anal. Biochem. 182 (1989) 16–19. https://doi.org/10.1016/0003-2697(89)90710-0.

[30] T. Mosmann, Rapid colorimetric assay for cellular growth and survival: application to proliferation and cytotoxicity assays., J. Immunol. Methods. 65 (1983) 55–63.

[31] E. Borenfreund, J.A. Puerner, Toxicity determined in vitro by morphological alterations and neutral red absorption, Toxicol. Lett. 24 (1985) 119–124. https://doi.org/10.1016/0378-4274(85)90046-3.

[32] M. Mohammadian, M. Salami, S. Momen, F. Alavi, Z. Emam-Djomeh, Fabrication of curcumin-loaded whey protein microgels: Structural properties, antioxidant activity, and in vitro release behavior, Lwt. 103 (2019) 94–100. https://doi.org/10.1016/j.lwt.2018.12.076.

[33] H. Ghaffari, M. Venkataramana, B. Jalali Ghassam, S. Chandra Nayaka, A. Nataraju, N.P. Geetha, H.S. Prakash, Rosmarinic acid mediated neuroprotective effects against H2O2-induced neuronal cell damage in N2A cells, Life Sci. 113 (2014) 7–13. https://doi.org/10.1016/j.lfs.2014.07.010.

[34] W. Hoyer, T. Antony, D. Cherny, G. Heim, T.M. Jovin, V. Subramaniam, Dependence of α-synuclein aggregate morphology on solution conditions, J. Mol. Biol. 322 (2002) 383–393. https://doi.org/10.1016/S0022-2836(02)00775-1.

[35] F. González-Lizárraga, S.B. Socías, C.L. Ávila, C.M. Torres-Bugeau, L.R.S. Barbosa, A. Binolfi, J.E. Sepúlveda-Díaz, E. Del-Bel, C.O. Fernandez, D. Papy-Garcia, R. Itri, R. Raisman-Vozari, R.N. Chehín, Repurposing doxycycline for synucleinopathies: Remodelling of α-synuclein oligomers

https://doi.org/10.1038/srep41755.

[36] W.E. Klunk, R.F. Jacob, R.P. Mason, Quantifying amyloid by congo red spectral shift assay, in: Methods Enzymol., Elsevier, 1999: pp. 285–305. https://doi.org/10.1016/S0076-6879(99)09021-7.

[37] W.E. Klunk, J.W. Pettegrew, D.J. Abraham, Quantitative evaluation of Congo red binding to amyloid-like proteins with a beta-pleated sheet conformation, J. Histochem. Cytochem. 37 (1989) 1273–1281. https://doi.org/10.1177/37.8.2666510.

[38] C. Mohanty, M. Das, S.K. Sahoo, Emerging role of nanocarriers to increase the solubility and bioavailability of curcumin, Expert Opin. Drug Deliv. 9 (2012) 1347–1364. https://doi.org/10.1517/17425247.2012.724676.

[39] Y. Fu, X. Gao, Y. Wan, J. Zhang, D. Kong, Z. Wang, Y. Zhao, Dendritic nanoconjugate containing optimum folic acid for targeted intracellular curcumin delivery, RSC Adv. 4 (2014) 46020–46023. https://doi.org/10.1039/c4ra08315f.

[40] K. Jain, P. Kesharwani, U. Gupta, N.K. Jain, Dendrimer toxicity: Let's meet the challenge, Int. J. Pharm. 394 (2010) 122–142. https://doi.org/10.1016/j.ijpharm.2010.04.027.

[41] P. Kolhe, E. Misra, R.M. Kannan, S. Kannan, M. Lieh-Lai, Drug complexation, in vitro release and cellular entry of dendrimers and hyperbranched polymers, Int. J. Pharm. 259 (2003) 143–160. https://doi.org/10.1016/S0378-5173(03)00225-4.

[42] A.A. D'Archivio, M.A. Maggi, Investigation by response surface methodology of the combined effect of pH and composition of water-methanol mixtures on the stability of curcuminoids, Food Chem. 219 (2017) 414–418. https://doi.org/10.1016/j.foodchem.2016.09.167.

[43] T. Chumroenphat, I. Somboonwatthanakul, S. Saensouk, S. Siriamornpun, Changes in curcuminoids and chemical components of turmeric (Curcuma longa L.) under freeze-drying and low-temperature drying methods, Food Chem. 339 (2021) 128121. https://doi.org/10.1016/j.foodchem.2020.128121.

[44] K.I. Priyadarsini, The chemistry of curcumin: From extraction to therapeutic agent, Molecules. 19 (2014) 20091–20112. https://doi.org/10.3390/molecules191220091.

[45] L. Wang, X. Xu, Y. Zhang, Y. Zhang, Y. Zhu, J. Shi, Y. Sun, Q. Huang, Encapsulation of curcumin within poly(amidoamine) dendrimers for delivery to cancer cells, J. Mater. Sci. Mater. Med. 24 (2013) 2137–2144. https://doi.org/10.1007/s10856-013-4969-3.

[46] R. Jagannathan, P.M. Abraham, P. Poddar, Temperature-dependent spectroscopic evidences of curcumin in aqueous medium: A mechanistic study of its solubility and stability, J. Phys. Chem. B. 116 (2012) 14533–14540. https://doi.org/10.1021/jp3050516.

[47] S.M. Khopde, K. Indira Priyadarsini, D.K. Palit, T. Mukherjee, Effect of Solvent on the Excited-state Photophysical Properties of Curcumin¶, Photochem. Photobiol. 72 (2007) 625–631.

[48] J. Cao, H. Zhang, Y. Wang, J. Yang, F. Jiang, Investigation on the interaction behavior between curcumin and PAMAM dendrimer by spectral and docking studies, Spectrochim. Acta - Part A Mol. Biomol. Spectrosc. 108 (2013) 251–255. https://doi.org/10.1016/j.saa.2013.02.003.

[49] B. Boruah, P.M. Saikia, R.K. Dutta, Binding and stabilization of curcumin by mixed chitosan-surfactant systems: A spectroscopic study, J. Photochem. Photobiol. A Chem. 245 (2012) 18–27. https://doi.org/10.1016/j.jphotochem.2012.07.004.

[50] A. Dutta, B. Boruah, A.K. Manna, B. Gohain, P.M. Saikia, R.K. Dutta, Stabilization of diketo tautomer of curcumin by premicellar anionic surfactants: UV-Visible, fluorescence, tensiometric and TD-DFT evidences, Spectrochim. Acta - Part A Mol. Biomol. Spectrosc. 104 (2013) 150–157. https://doi.org/10.1016/j.saa.2012.11.048.

[51] Y. Manolova, V. Deneva, L. Antonov, E. Drakalska, D. Momekova, N. Lambov, The effect of the water on the curcumin tautomerism: A quantitative approach, Spectrochim. Acta - Part A Mol. Biomol. Spectrosc. 132 (2014) 815–820. https://doi.org/10.1016/j.saa.2014.05.096.

[52] A. Abderrezak, P. Bourassa, J.S. Mandeville, R. Sedaghat-Herati, H.A. Tajmir-Riahi, Dendrimers bind antioxidant polyphenols and cisplatin drug, PLoS One. 7 (2012) e33102. https://doi.org/10.1371/journal.pone.0033102.

[53] A. Rohman, Sudjadi, Devi, D. Ramadhani, A. Nugroho, Analysis of curcumin in curcuma longa and Curcuma xanthorriza using FTIR spectroscopy and chemometrics, Res. J. Med. Plant. 9 (2015) 179–186. https://doi.org/10.3923/rjmp.2015.179.186.

[54] D.A. Tomalia, A.M. Naylor, W.A. Goddard, Starburst Dendrimers: Molecular-Level Control of Size, Shape, Surface Chemistry, Topology, and Flexibility from Atoms to Macroscopic Matter, Angew. Chemie Int. Ed. English. 29 (1990) 138–175. https://doi.org/10.1002/anie.199001381.

[55] D.E. Ybarra, M.N. Calienni, L.F.B. Ramirez, E.T.A. Frias, C. Lillo, S. del V. Alonso, J. Montanari, F.C. Alvira, Vismodegib in PAMAM-dendrimers for potential theragnosis in skin cancer, OpenNano. 7 (2022) 100053. https://doi.org/10.1016/j.onano.2022.100053.

[56] T.T. Win-Shwe, H. Sone, Y. Kurokawa, Y. Zeng, Q. Zeng, H. Nitta, S. Hirano, Effects of PAMAM dendrimers in the mouse brain after a single intranasal instillation, Toxicol. Lett. 228 (2014) 207–215. https://doi.org/10.1016/j.toxlet.2014.04.020.

[57] Y.J. Wang, M.H. Pan, A.L. Cheng, L.I. Lin, Y.S. Ho, C.Y. Hsieh, J.K. Lin, Stability of curcumin in buffer solutions and characterization of its degradation products, J. Pharm. Biomed. Anal. 15 (1997) 1867–1876. https://doi.org/10.1016/S0731-7085(96)02024-9.

[58] C.F. Lin, K.H. Yu, C.P. Jheng, R. Chung, C.I. Lee, Curcumin reduces amyloid fibrillation of prion protein and decreases reactive oxidative stress, Pathogens. 2 (2013) 506–519.

[59] K.M. Kitchens, R.B. Kolhatkar, P.W. Swaan, N.D. Eddington, H. Ghandehari, Transport of poly(amidoamine) dendrimers across Caco-2 cell monolayers: Influence of size, charge and fluorescent labeling, Pharm. Res. 23 (2006) 2818–2826. https://doi.org/10.1007/s11095-006-9122-2.

[60] O.P. Perumal, R. Inapagolla, S. Kannan, R.M. Kannan, The effect of surface functionality on cellular trafficking of dendrimers, Biomaterials. 29 (2008) 3469–3476. https://doi.org/10.1016/j.biomaterials.2008.04.038.

[61] C.J. Morris, G. Aljayyoussi, O. Mansour, P. Griffiths, M. Gumbleton, Endocytic Uptake, Transport and Macromolecular Interactions of Anionic PAMAM Dendrimers within Lung Tissue, Pharm. Res. 34 (2017) 2517–2531. https://doi.org/10.1007/s11095-017-2190-7.

[62] J. Yi, H. Huang, Y. Liu, Y. Lu, Y. Fan, Y. Zhang, Fabrication of curcumin-loaded pea protein-pectin ternary complex for the stabilization and delivery of β-carotene emulsions, Food Chem. 313 (2020) 126118. https://doi.org/10.1016/j.foodchem.2019.126118.

[63] T. Ak, I. Gülçin, Antioxidant and radical scavenging properties of curcumin, Chem. Biol. Interact. 174 (2008) 27–37. https://doi.org/10.1016/j.cbi.2008.05.003.

[64] L. Qi, J. Jiang, J. Zhang, L. Zhang, T. Wang, Curcumin protects human trophoblast HTR8/SVneo cells from H2O2-induced oxidative stress by activating nrf2 signaling pathway, Antioxidants. 9 (2020). https://doi.org/10.3390/antiox9020121.

[65] M. Rakotoarisoa, B. Angelov, V.M. Garamus, A. Angelova, Curcumin- and Fish Oil-Loaded Spongosome and Cubosome Nanoparticles with Neuroprotective Potential against H 2 O 2 -Induced Oxidative Stress in Differentiated Human SH-SY5Y Cells, ACS Omega. 4 (2019) 3061–3073. https://doi.org/10.1021/acsomega.8b03101.

[66] N. Oddone, N. Lecot, M. Fernández, A. Rodriguez-Haralambides, P. Cabral, H. Cerecetto, J.C. Benech, In vitro and in vivo uptake studies of PAMAM G4.5 dendrimers in breast cancer, J. Nanobiotechnology. 14 (2016) 1–12. https://doi.org/10.1186/s12951-016-0197-6.

[67] K. Milowska, M. Malachowska, T. Gabryelak, PAMAM G4 dendrimers affect the aggregation of α-synuclein, Int. J. Biol. Macromol. 48 (2011) 742–746. https://doi.org/10.1016/j.ijbiomac.2011.02.021.

[68] A. Rekas, V. Lo, G.E. Gadd, R. Cappai, S.I. Yun, PAMAM dendrimers as potentia] agents against fibrillation of α-Synuclein, a Parkinson's disease related protein, Macromol. Biosci. 9 (2009) 230–238. https://doi.org/10.1002/mabi.200800242.

[69] P. Alam, L. Bousset, R. Melki, D.E. Otzen, A-Synuclein Oligomers and Fibrils: a Spectrum of Species, a Spectrum of Toxicities, J. Neurochem. 150 (2019) 522–534. https://doi.org/10.1111/jnc.14808.